



**HAL**  
open science

## Medium Voltage Shunt Reactor Design and Switching

Christian Ngnie Ngonseu, Marc Petit, Martin Hennebel, Didier Larraillet,  
Fabien Petit

► **To cite this version:**

Christian Ngnie Ngonseu, Marc Petit, Martin Hennebel, Didier Larraillet, Fabien Petit. Medium Voltage Shunt Reactor Design and Switching. 2023 IEEE PES Innovative Smart Grid Technologies Conference Europe (ISGT-Europe), In press. hal-04276799

**HAL Id: hal-04276799**

**<https://hal.science/hal-04276799>**

Submitted on 9 Nov 2023

**HAL** is a multi-disciplinary open access archive for the deposit and dissemination of scientific research documents, whether they are published or not. The documents may come from teaching and research institutions in France or abroad, or from public or private research centers.

L'archive ouverte pluridisciplinaire **HAL**, est destinée au dépôt et à la diffusion de documents scientifiques de niveau recherche, publiés ou non, émanant des établissements d'enseignement et de recherche français ou étrangers, des laboratoires publics ou privés.

# Medium Voltage Shunt Reactor Design and Switching

Christian NGNIE NGONSEU  
GeePs | Group of electrical engineering  
- Paris  
CentraleSupélec, Université Paris  
Saclay  
Gif-sur-Yvette, France  
christian.ngonseu@centralesupelec.fr

Marc PETIT  
GeePs | Group of electrical engineering  
- Paris  
CentraleSupélec, Université Paris  
Saclay  
Gif-sur-Yvette, France  
marc.petit@centralesupelec.fr

Martin HENNEBEL  
GeePs | Group of electrical engineering  
- Paris  
CentraleSupélec, Université Paris  
Saclay  
Gif-sur-Yvette, France  
martin.hennebel@centralesupelec.fr

Didier LARRAILLET  
Ingénieur électrotechnique  
SRD  
Poitiers, France  
didier.larraillet@srd-energies.fr

Fabien PETIT  
Ingénieur électrotechnique  
SRD  
Poitiers, France  
fabien.petit@srd-energies.fr

**Abstract**—This paper presents a method for the sizing of a gapped-core nonlinear shunt reactor used for mitigation of overvoltages in a medium voltage distribution network with a high level of distributed generation. The study of the transient phenomena that occurs during reactor switching-in is also carried out. These phenomena include (i) inrush currents during switching due to saturation of the magnetic core, which is a silicon-steel (SiFe) iron core, and (ii) also the resulting voltage drop due to these high currents. The study shows the design a 1.4 Mvar shunt reactor with steps of 0.2 Mvar and presents inrush currents for the various steps.

**Index Terms**—Shunt reactor, reactive power, electromagnetic transient, saturation, inrush current, medium voltage (MV)

## I. INTRODUCTION

The high variability and uncertainty introduced in modern power distribution systems due to decentralized renewable energy generators requires new solutions for grid management and power quality assurance. DSO should be able to guarantee at all instant a voltage level in the range of  $0.95 \text{ p.u.} \leq V_{\max\_node} \leq 1.05 \text{ p.u.}$  on the medium voltage network and  $0.90 \text{ p.u.} \leq V_{\max\_node} \leq 1.10 \text{ p.u.}$  on the low voltage network [1]. In the present paper we focus on the overvoltage constraints resulting from the integration of photovoltaic generation into the existing grid and the installation of underground cables which produces much more reactive power than overhead lines. This issue is likely to become more frequent in the future with the expected growth of local generation. It will be a key issue for the DSOs who need to optimize their investments and must be enablers of the distributed generation development. The solution investigated is the use of shunt reactors to mitigate overvoltages. [2] They are widely used in transmission networks and they can also provide a solution for voltage control in distribution systems as well.

The sizing of an iron core shunt reactor with airgap is studied in [3], [4], [5]. A proposed model for reactor sizing is going to be detailed here, with the analysis of inrush currents during switching-in, and the resulting voltage drop.

Considering a sinusoidal voltage source  $e(t)$ , when energizing the reactor, the flux  $\phi(t)$  will evolve with the voltage such that

$$e(t) = E\sqrt{2}\sin(\omega t + \theta_0) \quad (1)$$

$$\int_{t=0}^t d\phi = \int_{t=0}^t e(t) dt \quad (2)$$

Let's note  $\phi_m$  the maximum flux in steady state, then the peak flux  $\phi_{peak}$  during the energization depends on the switching time and on the residual flux.

If energizing is done at the zero crossing of the voltage, the peak flux is equal to twice the maximum flux plus the residual flux  $\phi_r$ .

$$\theta_0 = 0 \quad \phi_{peak} = \phi_r + 2\phi_m \quad (3)$$

On the other hand, if the energizing is done at the maximum voltage, the peak flux is equal to the maximum flux plus the residual flux.

$$\theta_0 = \frac{\pi}{2} \quad \phi_{peak} = \phi_r + \phi_m \quad (4)$$

Figure 1 below (as described in [5]) shows the variation of the flux generated according to the switching time of the shunt reactor with respect to the supply voltage.

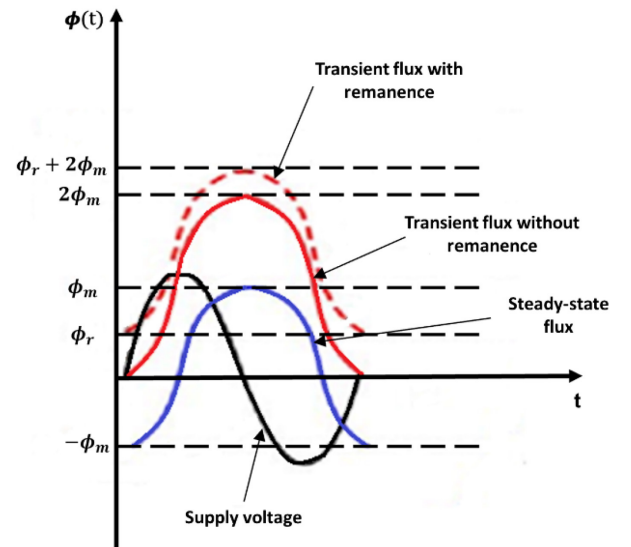


Figure 1 : Voltage - Flux variations for a ferromagnetic core [5]

## II. SIZING OF SHUNT REACTOR

### A. Determination of the number of turns and core cross section

The reactors have ferromagnetic cores with integrated air gaps. Due to these air gaps, the cores cannot be significantly saturated, and will have a reasonably linear behavior during switching-in events. Sizing with air gaps allows for reasonable physical characteristics, limits core saturation, therefore reduces reactor iron losses with lower remanent flux. Figure 2 shows the three arms of the core with equally sized air gaps with the turns wound around the core.

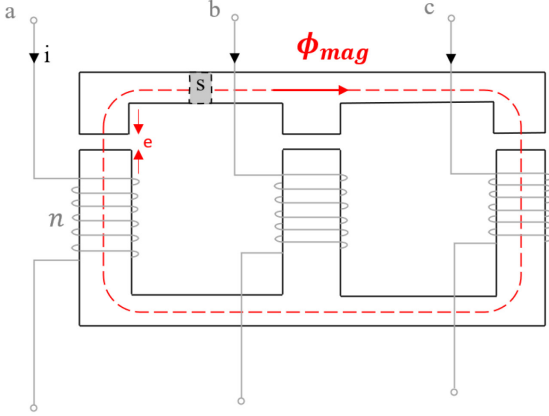


Figure 2 : Magnetic core with air gap

To determine the current-flux characteristics of the magnetic material it is necessary to determine the number of turns and the cross section of the iron core. The inductance value is defined from the requested reactive power given by;

$$L\omega = \frac{U^2}{Q} \quad (5)$$

$$\mathcal{R} = \frac{n^2}{L} \quad (6)$$

Where  $L$  is the inductance,  $Q$  the reactor's reactive power available,  $U$  the grid voltage,  $n$  the number of turns,  $\mathcal{R}$  the magnetic reluctance, and  $\omega$  the angular frequency.

To determine the number of turns we start from Ampere's law considering the difference of the flux intensity in the ferromagnetic core and in the air.

$$H_{iron} * l_e + H_{air} * e = n * i \quad (7)$$

$$B_{iron} = B_{air} \quad (8)$$

Where  $H_{iron}$  and  $H_{air}$  are the magnetic field intensity in the iron core and in air respectively,  $B_{iron}$  and  $B_{air}$  the magnetic flux density,  $l_e$  the field length,  $e$  the length of the airgap and  $i$  the current flowing in the turns.

From the reluctance in (6) and magnetomotive force in (7), we obtain the following relationship between the flux and current in the coils;

$$n * i = \mathcal{R} * \varphi = \mathcal{R} * B_{air} * s \quad (9)$$

$$\mathcal{R} = \frac{\frac{l_e}{\mu_r} + e}{\mu_0 s} = \frac{e\mu_r + l_e}{\mu_0 \mu_r s} \quad (10)$$

The iron core used in this study is made of silicon-steel alloy with a cross-section  $s$  to be determined. The relative permeability  $\mu_r$  of iron-silicon is  $54 * 10^3$  at room temperature [6] and according to the size of the air gap we find that ;

$$\mathcal{R} = \frac{e}{\mu_0 s} \text{ with } l_e \ll e\mu_r \quad (11)$$

Typically for an air gap of 0.01 m, the magnetic field length is negligible compared to the product  $e\mu_r$  which will be;

$$e\mu_r \approx 500 \text{ m} \quad (12)$$

Finally, we find the number of turns necessary for reactive power level  $Q$  to be absorbed by the reactor is found as follows;

$$n = \sqrt{\frac{3 U * B}{2 Q}} * \left(\frac{e}{\mu_0}\right) \quad (13)$$

For  $l_e \ll e\mu_r$  and for a given reactor power level, the sizing factor is the air gap size. Optimization of the air gap size for a reactor power can be done to limit copper losses since the number of turns depends on the air gap size. The cross-section of the core is

$$s = \sqrt{\frac{2 U}{3 \omega * B * n}} \quad (14)$$

Table 1 below summarises the number of turns and the core cross-sections determined for the different reactor sizes. These parameters allow to find the flux-current characteristics of the reactors. The dimensions are physically realisable.

Table 1 : Number of turns and core cross section

Q [Mvar]	Inductance L [H]	Turns [n]	Cross-section S [m <sup>2</sup> ]
0.2	6.37	1023	0.05
0.4	3.18	512	0.10
0.6	2.12	341	0.16
0.8	1.59	255	0.21
1	1.27	204	0.26
1.4	0.91	146	0.37

### B. Flux-current characteristics

The magnetization curve is plotted for a maximum magnetic induction of 1.5 T. The magnetic field intensity defined at the beginning of the saturation is given by;

$$H_{sat\_start} = B_{sat\_start} / (\mu_0 \mu_r) \quad (15)$$

A good approximation of the curve for saturation is the hyperbolic tangent [7] defined for the beginning of saturation and the maximum saturation;

$$a = \text{atanh}(B_{sat\_start} / B_{sat}) / H_{sat\_start} \quad (16)$$

$$B_{nonlinear} = B_{sat} * \tanh(a * H_{nonlinear}) \quad (17)$$

Where 'a' is non-linearity coefficient between  $B_{\text{sat\_start}}$  and  $B_{\text{sat}}$ ,  $H_{\text{nonlinear}}$  is the field defined with respect to the beginning of saturation.

Figure 3 is the saturation curve obtained from MATLAB implementation for a ferromagnetic iron-silicon material with a permeability of  $54 * 10^3$ .

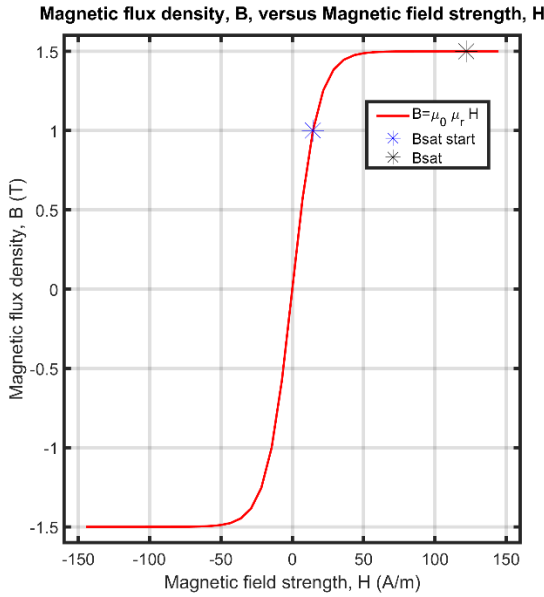


Figure 3 : Theoretical saturation curve silicon steel

From Ampere's theorem we deduce that

$$I_{\text{nonlinear}} = \frac{\mu_r * e}{n} * H_{\text{nonlinear}} \quad (18)$$

$$\phi_{\text{nonlinear}} = B_{\text{nonlinear}} * s * n \quad (19)$$

Figure 4 below gives the flux/current characteristics for 4 steps of reactor power. These characteristics are used to model the nonlinear behaviour of inductance in a Simulink model.

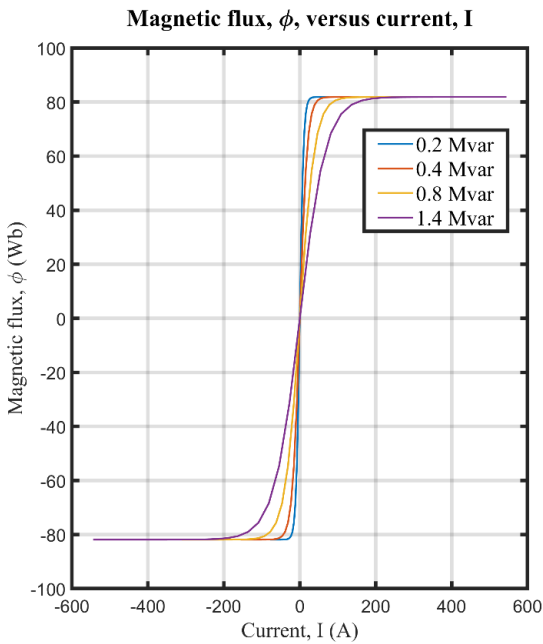


Figure 4 : Flux- current saturation curves for reactor sizes

### III. INRUSH CURRENT AT REACTOR ENERGIZATION

The calculation of switching transients requires proper modeling of the nonlinear flux-current curve of the reactor for a given reactive power. The nonlinearity is caused by the magnetization characteristics of the iron core of the shunt reactor. [8]

#### A. Simulink reactor model

The model presented in Figure 5 is that of a three-phase shunt reactor design inspired from a model proposed by the Center of Excellence for Transformers [8] which realized a 100 Mvar nonlinear shunt reactor for the Croatian network.

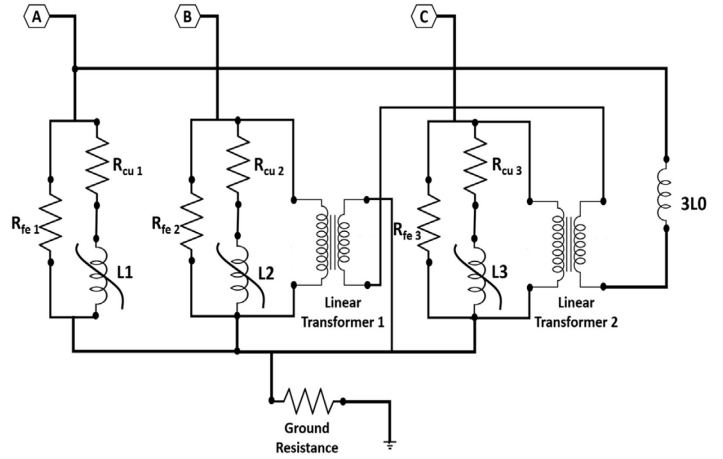


Figure 5 : Non-linear shunt reactor model

Each phase of the three-phases of the reactor is modelled as a nonlinear inductance L, with a series-connected resistor  $R_{\text{cu}}$  representing the copper losses of equal values for the three branches. A good approximation of the value of this resistance is the estimate of the length of the turns  $l_{\text{cu}}$  around a square core and a copper section  $S_{\text{cu}}$  of the turns necessary to support the nominal current of the reactor.

$$l_{\text{cu}} = 1.1 * 4l \quad (20)$$

$$R_{\text{cu}} = \rho \frac{l_{\text{cu}}}{S_{\text{cu}}} \quad (21)$$

A resistance  $R_{\text{Fe}}$ , connected in parallel, represents the iron losses. At low frequencies (50 Hz) the iron losses are negligible compared to the copper losses since the iron losses are more important at high frequencies according to the Steinmetz equation. Typically, for a 2000 kVA MV transformer, the iron losses are 0.13% [9]. For the purpose of the simulation, a high resistance represents  $R_{\text{Fe}}$ . The magnetic coupling between the three star-connected phases is represented by linear transformers with a transformation ratio of 1 and a zero-sequence inductance  $L_0$  that provides a path for the zero-sequence current.

#### B. Inrush current for a 1.4 Mvar reactor

The actual magnitude of the inrush current due to the energization of the reactor depends on the linearity range of the core and the instant of switching as described in the introduction. Connection operations at times close to zero voltage can cause inrush currents which can reach high amplitudes and have long time constants. Beyond the saturation point, the current increases much faster than the flux. Figure 6 shows the inrush current observed during switching at zero-voltage and the peak current is 710 A on

phase B. Figure 7 shows the inrush current for a maximum voltage switching. The peak current on phase B at this instant is 54 A.

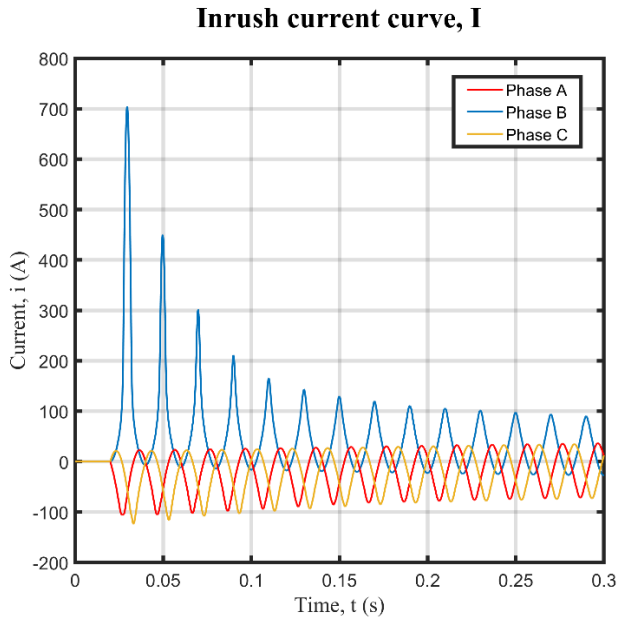


Figure 6 : Inrush current for switching in at  $V = 0 V$  on phase B

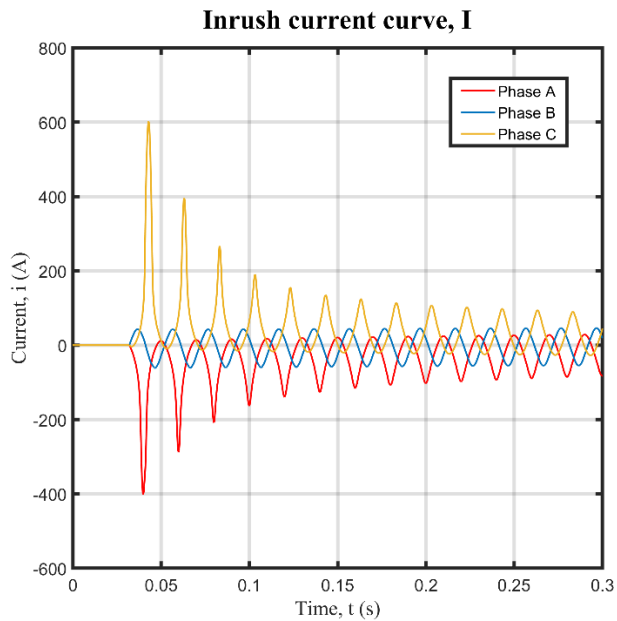


Figure 7 : Inrush current for switching in at  $V = V_{max} V$  on phase B

#### IV. CASE STUDY: REACTIVE POWER COMPENSATION VOLTAGE CORRECTION ON MV NETWORK

The DSO proposed three sizes (reactive power level) for the shunt reactors that are required to mitigate the overvoltages on the network. The reactors are connected to three nodes with reactive power of 1.4 Mvar at node 2 and node 3, and 0.4 Mvar at node 3. An optimisation was carried out with the PSO (particle swarm optimisation) algorithm to identify the point of connexion of the reactors. Figure 8 shows the network studied and the point of connection of the reactors.

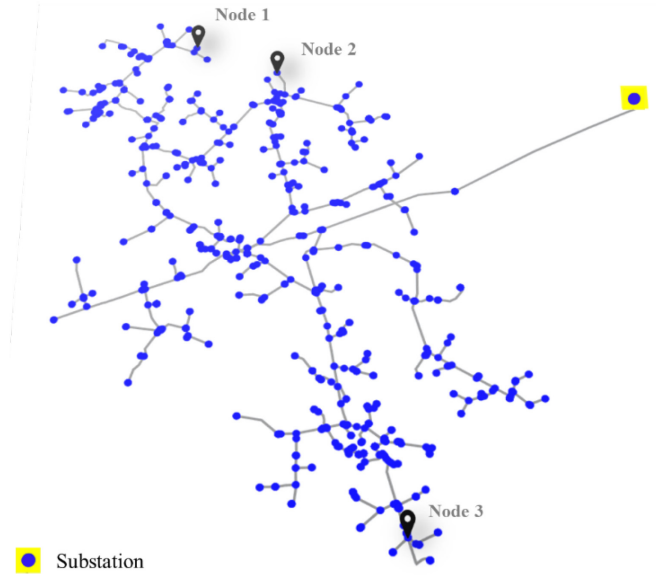


Figure 8: Point of connection of shunt reactors on the network studied

##### A. Reactor energization

The network was modelled on MATLAB Simulink with an operating point for renewable energy production set at 100 % of generation capacity (5.14 MW) and power consumption at 4 % of client subscribed power (18.25 MW). This configuration corresponds to the most constraining voltage rise situation and if overvoltages are corrected for this operating point, then they will be corrected for less constraining points. All the reactor steps are switched-in in the results presented here. For intermediate production/consumption levels, the reactor power levels are switched-in in accordance. The non-linear reactors are studied on this network to verify their power levels, the correction of overvoltages and also the voltage dips when they are energized. The switching-in on the three phases is done at  $t = 60$  ms. Table 2 below shows the voltage measured on each node on which the reactors are connected before and after switching-in.

Table 2 : Node voltages before and after reactor switching

	Node 1	Node 2	Node 3
Voltage without reactors V p.u.	1.056	1.061	1.066
Voltage with reactors V p.u.	1.006	1.009	1.005

Figure 9 shows the measured reactive power at the substation without reactors for  $t < 60$  ms and with reactors switched in for  $t > 60$  ms. The difference in reactive power measured after switching-in is 3.29 Mvar. This power corresponds to the sum of the reactive powers consumed by the reactors. This measurement validates the sizing and it verifies that the power absorbed on the nodes to which the reactors are connected correct the overvoltages.

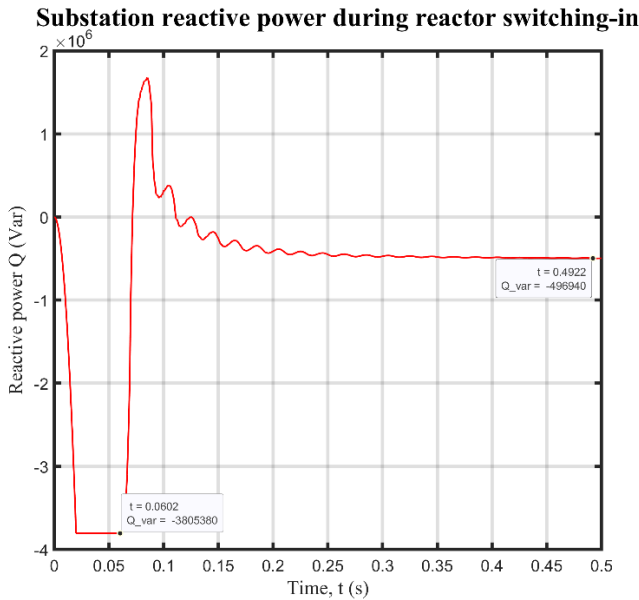


Figure 9 : Reactive power at substation

### B. Measurement of voltage dips

The voltage dip is generally defined as a drop from 10% to nearly 100% of the nominal voltage value for a time between 10 ms and a few seconds. As the inrush current is high, it is necessary to check that this current does not cause a voltage dip of more than 5% of the nominal voltage;

$$V_{reactor\_node} \geq 0.95pu \quad (22)$$

The reactor step that is the most constraining to engage is the step at 0.2 Mvar because the inductance is the most important as specified in Table 1. Figure 10 shows the RMS value of the voltage (calculated through a sliding period of 20 ms) on phase A for a step of 0.2 Mvar on a feeder node. There is a voltage drop on phase A and C at reactor switching-in and for a duration of 100 ms. The voltage limit is respected.

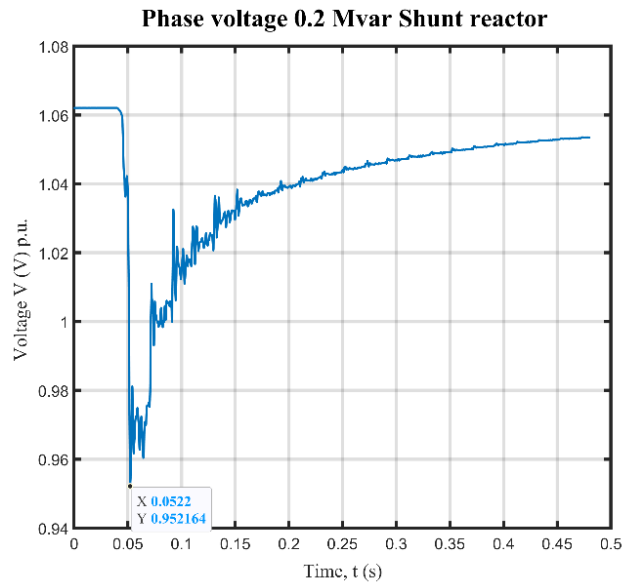


Figure 10: The normalised single-phase voltage

## V. CONCLUSION

This study focuses on the optimization of smart distribution networks. Due to the increasing presence of decentralised energy production and underground cables on these networks DSOs are facing more overvoltage issues. In this paper, a methodology is presented for the design of gapped-core shunt reactor used for correction of overvoltages in distribution networks. From a theoretical B-H curve for silicon steel, it was possible to derive the flux-current characteristics for rated shunt reactor powers. These characteristics implemented in a Simulink model and tested on a on distribution network gives rise to a peak current of 710 A when switching-in at  $V = 0$  V and no saturation current when switching-in is at  $V = V_{max}$  with  $I_{peak} = 54$  A measured on phase B. The voltage dip resulting from saturation current did not exceed voltage limit during reactor switching-in. The models of non-linear reactors designed here meet the expectations, the power levels for which they are dimensioned are respected. This approach can be used to design higher power shunt reactors.

## REFERENCES

- [1] European norm NF EN 50160 "Characteristic of the voltage supplied by the public distribution networks" February 2011
- [2] Schneider électrique "Medium Voltage distribution" 2022
- [3] Abbas Lotfi and Mohsen Faridi "Design Optimization of Gapped-Core Shunt Reactors" in IEEE Transactions on Magnetics, vol. 48, no. 4, pp. 1673-1676, April 2012
- [4] HSU MON AUNG1, DR. MIN MIN OO "Design of 25 MVA Shunt Reactor for 230 kV Transmission Line" in International Journal of Scientific Engineering and Technology Research, ISSN 2319-8885, vol.03, Issue.11, pp 2481-2486, June 2014
- [5] Z. Gaji, B. Hillström, et F. Meki, "HV shunt reactor secrets for protection engineers" ABB Sweden, presented to 30th Western Protective Relaying Conference p. 30. Octobre 2003
- [6] Jean-Claude BAVAY, Jean VERDUN "ALLIAGE FER SILICIUM" Technique de l'ingénieur Réf. : D2110 V1 December 1991
- [7] "Matlab simulink inbuilt model Custom Inductor (B-H Curve)" Matlab R2022b
- [8] Božidar Filipović-Grčića, Bojan Franca, Ivo Uglešića, Ivica Pavića, Samir Keitoub, Ivan Muratb, Igor Ivanković "Monitoring of transient overvoltages on the power transformers and shunt reactors – field experience in the Croatian power transmission system" in ScienceDirect Procedia Engineering, Volume 202, Pages 29-42, ISSN 1877-7058 May 2017
- [9] "2018 Schneider Electric distribution transformer catalog p 62"